

## Inversion of Chladni patterns by tuning the vibrational acceleration

Henk Jan van Gerner,<sup>1,\*</sup> Martin A. van der Hoef,<sup>1</sup> Devaraj van der Meer,<sup>1</sup> and Ko van der Weele<sup>2</sup>  
<sup>1</sup>*Faculty of Science and Technology and J.M. Burgers Centre for Fluid Dynamics, University of Twente, P.O. Box 217,  
 7500 AE Enschede, The Netherlands*

<sup>2</sup>*Department of Mathematics, University of Patras, 26500 Patras, Greece*  
 (Received 25 March 2010; published 22 July 2010)

Inverse Chladni patterns, i.e., grains collecting at the *antinodes* of a resonating plate, are traditionally believed to occur only when the particles are small enough to be carried along by the ambient air. We now show—theoretically and numerically—that air currents are *not the only* mechanism leading to inverse patterns: When the acceleration of the resonating plate does not exceed  $g$ , particles will always roll to the antinodes, irrespective of their size, even in the absence of air. We also explain why this effect has hitherto escaped detection in standard Chladni experiments.

DOI: 10.1103/PhysRevE.82.012301

PACS number(s): 45.70.-n, 05.65.+b, 47.11.-j

*Introduction.* A classic way of visualizing standing waves is by sprinkling sand or salt on a horizontal plate and bring it into resonance by, e.g., a violin bow. The particles will move to the nodal lines, giving rise to the famous Chladni patterns, by now a standard high-school demonstration experiment [1,2]. Much less known is that very fine particles will move to the *antinodes*: This was already noted by Chladni himself, who observed that tiny hair shavings from his violin bow were carried to the antinodes, and systematically studied by Faraday with the use of lycopodium powder [3]. He and others showed that the inverse Chladni patterning of fine particles is due to air currents induced by the vibrating plate [3–6], which drag the particles along to the antinodes.

In this paper we give a proof-of-principle that *all* particles—also large ones for which the effect of air can be ignored—are able to form inverse Chladni patterns, by a completely different mechanism: If the vibrational acceleration of the plate remains below  $g$ , their movement due to the vibration is directed toward the antinodes. In other words, one can switch from standard to inverted Chladni patterns simply by tuning the acceleration of the resonating plate. We demonstrate this analytically and confirm it by numerical simulation. We also propose how the phenomenon might be observed experimentally, which turns out to be difficult but not impossible.

*Numerical simulations.* The simulated system consists of a flexible rectangular plate on which 80 000 glass beads ( $\rho = 2.50 \times 10^3 \text{ kg/m}^3$ , diameter 1.0 mm) are uniformly distributed. The plate is fixed along its outer rim. We excite a standing wave pattern by applying one of the natural frequencies  $\omega_{kl}$  of the plate, corresponding to  $k$  sinusoidal half-wavelengths in the  $x$  direction and  $l$  in the  $y$  direction. Ignoring the additional bending of the plate under its own weight (we come back to this later), the vertical deflection at position  $(x, y)$  is then given by:

$$z(x, y, t) = a \sin(\omega_{kl}t) \sin \frac{k\pi x}{L_x} \sin \frac{l\pi y}{L_y}, \quad (1)$$

(with  $k, l = 1, 2, 3, \dots$ ), where  $a$  is the amplitude of the vibration and  $L_x = L_y = 62 \text{ cm}$  the size of the plate. As an example, in Fig. 1, we have excited the  $2 \times 2$  mode, which for a typical stainless steel plate of 1 mm thickness has a natural frequency of  $f_{22} (= \omega_{22}/2\pi) = 50 \text{ Hz}$  [9].

The trajectories of the particles are calculated via a Granular Dynamics code [7], in which the collisions (with the plate, and between the particles themselves) are taken care of by a three-dimensional soft sphere model including tangential friction. The results do not depend sensitively on the precise values of the coefficients of friction and (normal and tangential) restitution, which are set to 0.20, 0.90, and 0.33, respectively, both for the particle-plate and particle-particle interactions. Our key parameter is the dimensionless acceleration  $\Gamma = a\omega_{kl}^2/g$ , i.e., the ratio of the (maximal) vibrational and the gravitational acceleration. For a given mode, with a prescribed frequency  $\omega_{kl}$ , the value of  $\Gamma$  is varied via the amplitude  $a$ .

Figure 1(a) shows the final pattern when the plate is given

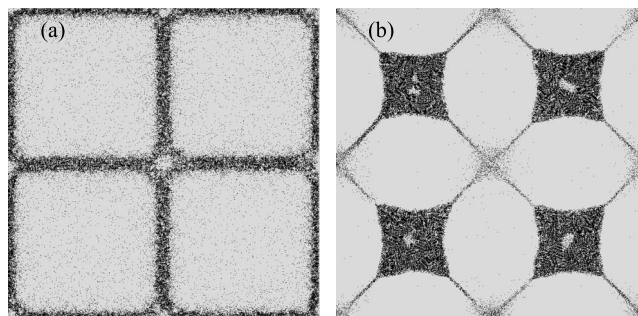


FIG. 1. (a) Top view of a flexible plate resonating in its  $2 \times 2$  mode, at 50 Hz, with an amplitude of 0.40 mm (dimensionless acceleration  $\Gamma = 4.0$ ). After 4 s most particles have collected at the nodal lines, forming a classic Chladni pattern. (b) The same plate at a smaller amplitude of 0.09 mm ( $\Gamma = 0.91$ ). The particles now migrate from the nodal lines to the anti-nodes and after 1 min an inverse Chladni pattern has formed. A movie of the formation process can be found in [8].

\*Present address: National Aerospace Laboratory, P.O. Box 153, 8300 AD Emmeloord, The Netherlands.

an amplitude of 0.40 mm ( $\Gamma=4.0$ ). In this case the local dimensionless acceleration is larger than unity over a sizeable region around the antinodes, with a maximum of 4.0 at the antinodes themselves. The particles in these regions start to bounce and the bounces tend (on average) to increase their kinetic energy. On the other hand, at the nodal lines the dimensionless acceleration is zero and the inelastic collisions with the plate *reduce* the kinetic energy of the particles; this effect is further enhanced by the mutual particle-particle collisions. Starting with all 80 000 particles uniformly distributed over the plate, within seconds most of them have migrated to the nodal lines, forming a standard Chladni pattern.

If we reduce the amplitude to  $a=0.09$  mm [ $\Gamma=0.91$ , Fig. 1(b)], the particles stop bouncing and start to *roll* toward the antinodes. The motion gradually speeds up and after about one minute most of the particles have accumulated at the antinodes, forming an inverse Chladni pattern. We have performed simulations also at other resonant frequencies, always with the same outcome: a standard pattern for  $\Gamma > 1$ , and an inverted one for  $\Gamma \leq 1$ . So the pattern can be tuned by amplitude only.

*Theory.* Why do the particles move to the antinodes for accelerations below 1 g, i.e., when they do not bounce? The explanation must lie in the fact that—as long as the particles remain in contact with the plate—the horizontal force on the particles, averaged over a complete vibration cycle, points toward the antinodes. In our analysis we assume the particles roll without slipping. We further ignore the influence of the ambient air, which is a good approximation for 1-mm glass spheres. Finally, we ignore the bending of the plate under its own weight and that of the particles, as well as the slight modification of the plate's resonant mode due to the presence of the particles [10].

For  $\Gamma \leq 1$  the particles do not detach from the plate and their vertical position is given by the same Eq. (1) as for the plate, except that  $x$  and  $y$  are now functions of time. For simplicity, let us for the moment only consider the  $x$  direction, so the vertical position of a particle is:

$$z(x,t) = a \sin(\omega_{kl}t) \sin \frac{k\pi x(t)}{L_x}, \quad k,l = 1,2,3, \dots \quad (2)$$

The up-and-down motion of the plate affects the particle's effective weight  $W$  [12]:

$$W(x,t) = -m[g + \ddot{z}(x,t)] \\ \approx -m \left[ g - a\omega_{kl}^2 \sin(\omega_{kl}t) \sin \frac{k\pi x(t)}{L_x} \right], \quad (3)$$

where  $m$  is the mass of the particle, and the minus sign indicates that  $W$  is a force pointing in the negative  $z$  direction. Its magnitude  $|W|$  oscillates around  $mg$ . It can be split in a component perpendicular to the plate  $W_{\perp}$ , which is counteracted by the normal force  $F_n$  on the particle, and a parallel component  $W_{\parallel}$ , which gives the particle an acceleration along the plate's surface.

The forces  $W_{\perp}$ ,  $F_n$ , and  $W_{\parallel}$  are shown in Fig. 2 at two different instants. In Fig. 2(a) the plate is accelerating upward at the location of the particle, so  $|W| > mg$ . In Fig. 2(b) it is accelerating downward, so now  $|W| < mg$ . As a result,

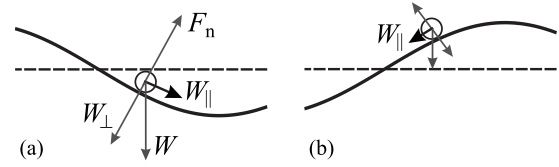


FIG. 2. The effective weight  $W$  of a particle on the resonating plate and the normal force  $F_n$  at two moments during a vibration cycle; the amplitude of the plate has been exaggerated for clarity. The component  $W_{\perp}$  and the normal force  $F_n$  balance each other, while the component  $W_{\parallel}$  gives the particle an acceleration along the plate's surface. It is larger in (a) than in (b) and hence the acceleration averaged over a complete vibration cycle is directed toward the antinodes.

the component parallel to the plate ( $W_{\parallel}$ ) is larger in Fig. 2(a) than in Fig. 2(b), hence the net acceleration over a complete cycle is directed to the antinodes. This is the origin of the inverse Chladni patterning.

Let us analyze this mechanism in some more detail. The parallel component of the force  $W_{\parallel} = W \sin \phi$ , with  $\phi$  the local angle of the plate with the horizontal, is approximately equal to  $W$  times the local slope of the plate ( $\sin \phi \approx \tan \phi = dz/dx$ ):

$$W_{\parallel}(x,t) \approx W(x,t) \frac{dz(x,t)}{dx} = W(x,t) \frac{k\pi a}{L_x} \sin(\omega_{kl}t) \cos \frac{k\pi x(t)}{L_x}, \quad (4)$$

and this gives the particle both a translational and rotational acceleration. The equation of motion for the translation is  $\Sigma F_{\parallel} = W_{\parallel} - f = ma_{\text{cm}}$  (with  $f$  the friction force with the plate, and  $a_{\text{cm}}$  the acceleration of the particle's center of mass), while the rotational motion is governed by  $\Sigma \tau = fr = I_{\text{cm}} \alpha$ , with  $\tau$  the torque exerted by the friction,  $r$  the particle radius,  $I_{\text{cm}} = \frac{2}{5}mr^2$  the particle's moment of inertia for rotation around its center of mass, and  $\alpha$  the angular acceleration [13]. Assuming that the particle rolls without slipping (i.e.,  $\alpha = a_{\text{cm}}/r$ ), the translational acceleration is given by:

$$a_{\text{cm}}(x,t) \equiv \ddot{x}(x,t) = \frac{5W_{\parallel}(x,t)}{7m}. \quad (5)$$

Substituting this result in the translational equation of motion, we also find the friction force:  $f = \frac{2}{7}W_{\parallel}$ . To ensure that the particle will not slip, the coefficient of static friction between them ( $\mu_s$ ) is able to deliver this force [14]. Since the maximum force of static friction equals  $\mu_s W_{\perp}$ , this means that we require  $\mu_s \geq f/W_{\perp} = \frac{2}{7}W \sin \phi / W \cos \phi = \frac{2}{7} \tan \phi$ . Since  $\phi$  always remains small, the above condition is easily fulfilled; e.g., steel beads on a steel plate ( $\mu_s = 0.74$ ) will do fine.

To calculate the average horizontal acceleration over a complete cycle, we must integrate Eq. (5) from  $t=0$  to  $2\pi/\omega_{kl}$ . Compared to the wavelength of the plate, the change in  $x$  position of a particle during one cycle is very small and we may treat  $x(t)$  as a constant. This gives:

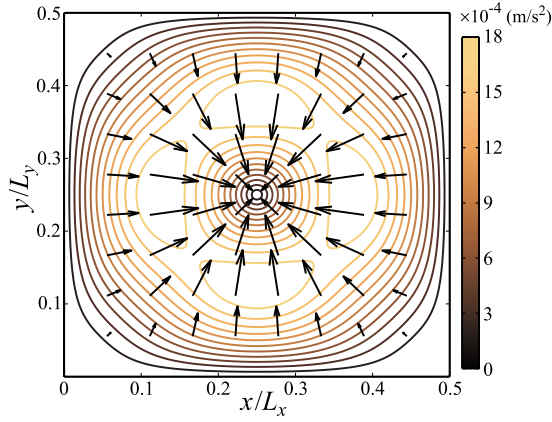


FIG. 3. (Color online) Time-averaged horizontal acceleration field experienced by beads rolling over a rectangular plate resonating in its  $2 \times 2$  mode for  $\Gamma=0.91$ , as in Fig. 1(b). Only one quarter of the plate is shown. The contour lines show the magnitude of the acceleration, also indicated by the length of the arrows. The acceleration field points to the antinode, explaining the formation of the inverse Chladni pattern.

$$\langle \ddot{x} \rangle(x,t) = \frac{\omega_{kl}}{2\pi} \int_0^{2\pi/\omega_{kl}} \ddot{x}(x,t) dt = \frac{5k\pi a^2 \omega_{kl}^2}{28L_x} \sin \frac{2k\pi x(t)}{L_x}, \quad (6)$$

where  $\Gamma = a\omega_{kl}^2/g$  is understood not to exceed 1. Note that the term of Eq. (3) involving  $g$  vanishes in the integration, reflecting the fact that the time-averaged contribution of gravity to the parallel acceleration is zero.

The acceleration in both directions  $x$  and  $y$  simultaneously can be derived in analogous manner, and Fig. 3 shows the average horizontal acceleration as a function of the position  $(x,y)$  for one quarter of the vibrating plate in the  $2 \times 2$  mode, in top view. The acceleration field is directed to the antinodes, and its magnitude is maximal somewhere midway between the nodes and antinodes. At the nodes and antinodes themselves the horizontal acceleration is zero. That is why the migration of particles beginning at the nodes [as in Fig. 1(b) and the accompanying video [8]] starts slowly, then speeds up, and finally comes to rest again at the antinodes [15].

Close inspection of Fig. 3 shows that the arrows are not pointing straight toward the anti-node (except on the diagonals): They are curving gently toward the four diagonal lines, bending around the four “islands” of maximal acceleration. Together with the regions of small acceleration near the nodal lines, this explains the observed diagonal migration channels in Fig. 1(b).

In order to quantitatively compare theory and numerical simulation, we carried out a simulation for 900 evenly distributed particles, initially at rest with respect to the plate. Owing to the limited number of particles and their uniform initial distribution, they do not collide with each other during the first 7 s (this is important for the comparison, since the analysis given above does not take into account collisions): The solid dots in Fig. 4 are the particle positions after 5 s of simulation, whereas the line crossings represent the theoret-

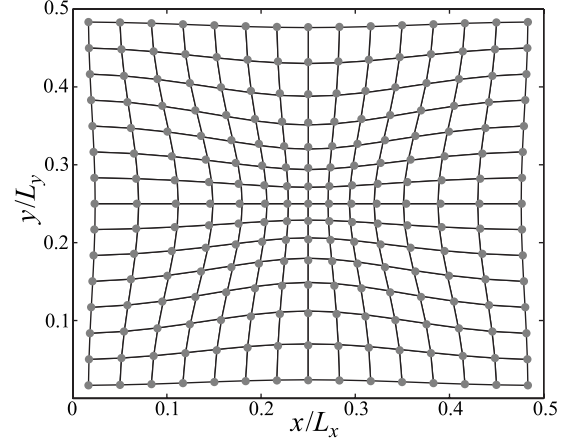


FIG. 4. Position of 225 particles after 5 s of vibration (starting out from a uniform distribution) on one quarter of a resonating plate in the  $2 \times 2$  mode at  $\Gamma=0.91$ . The grid line crossings represent the theoretically predicted positions [from Eq. (6) generalized to both the  $x$  and  $y$  direction], the dots are the positions obtained by numerical simulation.

cally predicted positions according to the  $(x,y)$ -version of Eq. (6). The correspondence is seen to be very good.

*Experimental considerations.* Our simulations and theoretical analysis show that inverse Chladni patterns are not reserved to fine dust particles that are swept along by the air currents around the resonating plate. Large beads (on which the air currents have no effect whatsoever) can form inverse Chladni patterns too. Why is it then that no one has ever reported this observation, even though the Chladni plate is a well-known and often conducted experiment? We discuss two important reasons.

The *first reason* stems from the fact that the plate must be perfectly horizontal: Even a small deviation may already outbalance the tiny vibration amplitudes imposed by the condition  $\Gamma < 1$  [typically one-tenth of a millimeter or less, cf. Figure 1(b)]. At the outer rims of the plate this is just a question of accurate alignment, but the horizontality is also affected by the bending of the plate under its own weight and that of the particles. Under normal circumstances, the deflection of the middle of the plate due to its own weight will be considerably larger than the largest admissible vibration amplitude  $a$ , so the particles will simply roll toward the center, overpowering any tendency to form inverse Chladni patterns.

The deflection for a square plate of dimensions  $L \times L$ , density  $\rho$ , and thickness  $h$  is given by [17]:

$$d_{\text{bend}} = 0.00406 \frac{g\rho h L^4}{D}, \quad (7)$$

where  $D = Eh^3/12(1-\nu^2)$  is the stiffness of the plate, with  $E$  the elastic modulus and  $\nu$  Poisson’s ratio [18]. This is to be compared with the largest admissible vibration amplitude  $a_{\text{max}} = g/\omega_{kl}^2$  (from the condition  $\Gamma < 1$ ), with the frequency of the  $k \times l$  mode being given by  $\omega_{kl} = (k^2 + l^2)\pi^2 L^{-2}(D/\rho h)^{1/2}$  [9], so

$$a_{\max} = \frac{1}{(k^2 + l^2)^2 \pi^4} \frac{g \rho h L^4}{D}. \quad (8)$$

Interestingly, the ratio  $R = d_{\text{bend}}/a_{\max} = 0.00406(k^2 + l^2)^2 \pi^4$  is independent of the material properties or plate dimensions: It only depends on the mode that is excited. For the  $2 \times 2$  mode one finds  $R = 25.3$ , and even for the  $1 \times 1$  mode the ratio is still 1.58 [19]. It is therefore necessary to experimentally suppress the deflection of the plate by raising the air pressure below the plate by an amount  $g \rho h$  N/m<sup>2</sup> (the plate's weight per square meter). Apart from that, it is preferable to work with a limited number of particles.

The *second reason* concerns the minimum force required to set a particle in rolling motion. This force is equal to  $\mu_r W_{\perp}$ , with  $\mu_r$  the coefficient of pre-rolling friction [20], so we require  $W_{\parallel} > \mu_r W_{\perp}$ . It is clearly advantageous to choose the particles and plate such that  $\mu_r$  is small, i.e., both of them should hardly deform. For steel particles on a steel plate its value is in the order of  $\mu_r = 0.002 - 0.003$ , if proper care is taken to eliminate disturbing effects such as the formation of liquid bridges due to humidity or a liquid film on particle and plate.

Now,  $W_{\perp}$  is approximately equal to  $mg$ , and for the parallel force we use  $W_{\parallel} = \frac{7}{5} m \langle \ddot{x} \rangle$  with  $\langle \ddot{x} \rangle$  given by Eq. (6). In

fact we use its maximum value, at the moments when  $\sin(4\pi x(t)/L_x) = 1$ , and with  $\Gamma = 1$ . The condition for setting the particles in rolling motion then takes the form  $k \pi g / 4L \omega_{kl}^2 \geq \mu_r$ . Inserting the expression for  $\omega_{kl}$  given above Eq. (8), this yields the following condition for the size of the plate:

$$L \geq \left[ \frac{4(k^2 + l^2)^2 \pi^3 D}{kg \rho h} \mu_r \right]^{1/3}. \quad (9)$$

For the  $2 \times 2$  mode ( $k = l = 2$ ) on a steel plate of thickness  $h = 1 \times 10^{-3}$  m (the same as in the simulations of Fig. 1) this is readily evaluated to give  $L \geq 10 \mu_r^{1/3}$  [18]. With  $\mu_r = 0.003$ , to be on the safe side, this means that the size of the plate must be at least  $1.45 \times 1.45$  m<sup>2</sup>.

The above requirements (the pressurization below the plate, and its large size) are demanding but not forbidding. It will be highly interesting to perform the experiment and witness the inverse Chladni patterning in real.

We thank Katherine Giannasi, Hans Kuipers, Detlef Lohse, and Hans-Jürgen Stöckmann for useful discussions. This work is part of the research program of FOM which is financially supported by NWO.

- 
- [1] H.-J. Stöckmann, *Physik Journal* **5**, 47 (2006); *Eur. Phys. J. Spec. Top.* **145**, 15 (2007).
- [2] E. F. F. Chladni, *Die Akustik (Breitkopf&Härtel, Leipzig, 1802); Traité d'Acoustique* (Courcier, Paris, 1809).
- [3] M. Faraday, *Philos. Trans. R. Soc. London* **121**, 299 (1831).
- [4] L. Rayleigh, *Philos. Trans. R. Soc. London* **175**, 1 (1884).
- [5] M. D. Waller, *Br. J. Appl. Phys.* **6**, 347 (1955).
- [6] M. Dorrestijn *et al.*, *Phys. Rev. Lett.* **98**, 026102 (2007).
- [7] M. A. van der Hoef *et al.*, *Adv. Chem. Eng.* **31**, 65 (2006).
- [8] See supplementary material at <http://link.aps.org/supplemental/10.1103/PhysRevE.82.012301> for a video showing the formation of the Chladni and inverse Chladni patterns of Fig. 1.
- [9] L. Meirovitch, *Analytical Methods in Vibrations* (Macmillan, New York, 1967).
- [10] The influence of their collective mass on the resonant mode may in fact give the particles some extra drive towards the antinodes. A related effect is observed in soap films excited by a sound wave, where the mass distribution (self-adapting the film's resonant mode to the excitation frequency) concentrates at the antinodes [11].
- [11] A. Boudaoud, Y. Couder, and M. Ben Amar, *Phys. Rev. Lett.* **82**, 3847 (1999); *Eur. Phys. J. B* **9**, 159 (1999); See also M. Brazovskaia and P. Pieranski, *Phys. Rev. Lett.* **80**, 5595 (1998); E. Leung *et al.*, *J. Acoust. Soc. Am.* **72**, 615 (1982); M. L. Cordero and N. Mujica, *ibid.* **121**, EL244 (2007).
- [12] We neglect the terms in  $\ddot{z}$  with amplitudes  $(2ka\pi/L_x)\dot{x}$ ,  $(2ka\pi^2/L_x^2)\dot{x}^2$ , and  $(k\pi/L_x)\ddot{x}$ . For  $k=2$  all these terms are much smaller than  $g$ .
- [13] See e.g. H. D. Young and R. A. Freedman, *Sears and Zemansky's University Physics*, 10th ed. (Addison-Wesley, San Francisco, 2000), Chap. 10-4, p. 305-306.
- [14] When a particle rolls without slipping, its point of contact with the plate is instantaneously at rest, so the friction force is a static (not a dynamic) one.
- [15] At first sight the mechanism described here is reminiscent of the drift of particles floating on a resonating water surface [16], which also happen to cluster in Chladni patterns, either standard or inverted ones. However, for floating particles the distinction between the two types of patterns is due to capillarity effects, *not* to a variation of  $\Gamma$ . Hydrophilic particles gather at the nodes of the water surface (forming a standard Chladni pattern), whereas hydrophobic particles go to the antinodes [16].
- [16] G. Falkovich *et al.*, *Nature (London)* **435**, 1045 (2005).
- [17] S. T. Timoshenko and S. Woinowsky-Krieger, *Theory of Plates and Shells* (McGraw-Hill, New York, 1959).
- [18] A stainless steel plate has density  $\rho = 7.8 \times 10^3$  kg/m<sup>3</sup> and stiffness  $D = 18.3$  kg m<sup>2</sup>/s<sup>2</sup> (elastic modulus  $E = 20 \times 10^{10}$  Pa, Poisson's ratio  $\nu = 0.30$ ).
- [19] The  $1 \times 1$  mode has only one antinode, at the center of the plate, so in this case the inverse-Chladni mechanism and the natural tendency to roll towards the lowest bending point both direct the particles to the central position. This makes the  $1 \times 1$  mode less suited to demonstrate the inverse Chladni patterning.
- [20] For rolling friction, similar as for sliding friction, the static pre-rolling coefficient exceeds the dynamic coefficient which holds when the particle is already rolling. See e.g. K. G. Budinski, *Wear* **259**, 1443 (2005); K. de Moerlooze and F. Al-Bender, *Adv. in Tribology Vol.* **2008**, 561280 (2008).